Estimation of the Torso Vibrotactile Thresholds using Eccentric Rotating Mass Motors

G. García-Valle, S. Arranz-Paraíso, I. Serrano-Pedraza, and M. Ferre, *Member, IEEE*

***Abstract*— The characterization of vibrotactile perception is crucial to accurately configure haptic devices and create appropriate stimuli for improving the user's performance in human-machine interaction systems. This paper presents a study aiming to determine the absolute and differential vibrotactile thresholds of the torso (front and back) to develop reliable haptic patterns to be displayed using a haptic vest. In the 'absolute threshold' experiment, we measured the minimum detectable vibration using a forced-choice task. In the 'differential threshold' experiment, we measured the minimum change needed for users to discriminate two successive vibrotactile stimuli using a vibration matching task. The results of the first experiment show similar absolute thresholds among areas, opening up the possibility to set a unique minimal vibration in order to create haptic patterns. On the other hand, the differential thresholds are generally similar between areas, which allow generalizing the results as well. Moreover, as the differential thresholds follow Weber's law, it is viable to estimate any upper or lower differential threshold for any reference frequency or amplitude. Our experiments thus prove the feasibility of creating vibrotactile patterns in a generalized manner for any area of the vest using ERM motors.**

***Index Terms*— Haptics, Perception and Psychophysics, Vibrotactile Feedback, Vibrotactile Thresholds, Haptic Patterns**

I. Introduction

HAPTICS is becoming an essential manner to improve the performance of numerous human-machine interaction applications such as virtual reality, navigation or spatial awareness systems. There already exist a high amount of devices implementing haptic actuation; but vibrotactile feedback, both tactile and kinesthetic, is doubtlessly the most widely used [1] [2] [3]. Tactile devices are commonly more portable and less bulky; thus, they are suitable for continuous usage, being capable of reproducing abundant stimuli using different actuators with an adequate configuration [4].

A human-machine system with vibrotactile feedback requires dependable stimuli, for instance, to simulate virtual events, or to create navigation cues to guide a person. Those interactions are simulated using haptic patterns composed of successive stimuli with shifting operating features (time, frequency, amplitude, etc.). If those patterns are rightly developed, users can associate the stimuli with the information that the haptic system attempts to convey. It is then required to characterize how users perceive vibrotactile stimuli by conducting psychophysical studies to determine the best manner to use the actuators, and create haptic stimuli [5] [6].

We previously developed a haptic vest which contains 72 Eccentric Rotating Mass (ERM) motors to render vibrotactile feedback, although it also contains thermal and impact actuation [4]. The motors had to meet some requisites: 1) ease to integrate alongside thermal and impact actuators in the vest; 2) low price owing to the large number of motors; 3) a small driver system not to increase the bulkiness and weight of the vest; 4) a wide range of operation to create versatile stimuli. Despite there are other actuators which have greater flexibility to handle their operating parameters (e.g. Linear Resonant Actuators [7]), the selected ERM motors are those which fulfil the four previous conditions.

Therefore, we needed to characterize tactile perception in the torso to use these ERM motors. To date, there barely are psychophysical studies employing ERM motors over the torso. Most of the research focuses on ascertaining the spatial acuity in specific areas [8] or other parameters over areas where the accuracy of tactile perception is usually greater [9] [10]. We then believe necessary to attain vibrotactile perception thresholds (both absolute and differential) to be able to create and render haptic patterns with a haptic vest. As a first step, in a previous study, we determined the vibrotactile spatial acuity (i.e. the distance between two operating actuators to perceive them as distinct stimuli) whose results were used to distribute the actuators over the vest [11].

In this research, we conduct two additional experiments: firstly, the determination of absolute vibrotactile thresholds (i.e. the minimum vibration detected through the skin) and, secondly, the determination of upper and lower differential thresholds so as to attain the minimum difference (among operating frequency or amplitude) to discriminate two distinct vibrations. Results of both experiments set a range of noticeable vibrations over the torso whose lower limit is the absolute vibration threshold, whereas the upper limit is the maximum vibration of the ERM motor. The resulting differential thresholds afford to define stimuli at each phase of a pattern so that users perceive every single stimulus, and the patterns convey information accurately.

We have divided the torso into 16 areas to ascertain

G. García-Valle, S. Arranz-Paraíso and M. Ferre are with the Center for Automation and Robotics (UPM-CSIC), Madrid, 28806, Spain (e-mail: m.ferre@upm.es, sandraar@ucm.es, gonzalo.gvalle@upm.es)

S. Arranz-Paraíso and I. Serrano-Pedraza are with the Faculty of Psychology, Complutense University of Madrid, Campus de Somosaguas, Pozuelo de Alarcón, Madrid, 28223, Spain (e-mail: sandraar@ucm.es, iserrano@ucm.es)

vibratory thresholds over the entire upper body, besides the differences between particular areas. If results are similar, the same haptic patterns can be created in a generalized manner for the whole torso and, otherwise, each specific area would need a customized design to convey the information properly.

In summary, both experiments yield reference values of frequency and amplitude which, along with the previous results of spatial acuity [11], allow creating easily perceivable and discriminable stimuli. The final objective is to enhance human-machine interactions systems by rendering patterns via a haptic vest, which are relatable to navigation or guidance cues, or to events coming from a virtual environment [4].

The outline of this paper is as follows: Section II describes the related work; Section III introduces the experimental setup consisting of the vibrotactile actuation system and the vest; Section IV describes the first experiment including the apparatus, the procedures, the statistical analysis, and the results; Section V presents the second experiment with the same subsections; Section VI discusses the results and compares them with prior studies, and Section VII sums up the main conclusions drawn from the conducted studies.

II. Related Work

Although the development of haptic devices and, consequently, of haptic patterns is rather recent, the study of vibrotactile sensory thresholds goes back several decades. There are even studies from the 60s dealing with these thresholds and how they are affected by some parameters such as temporal summation [12], masking [13] or actuation areas [14]. However, the technology has evolved substantially since then, acquiring more versatility and easiness to modify the operating conditions of vibrotactile actuators. Thereby, human perception must be newly characterized to set the required references to develop haptic feedback with current technology.

As mentioned before, most of researches about perception refer to fingers to determine either the spatial acuity [11] or the absolute and differential thresholds [15] [16]. Moreover, there are similar researches conducted over hands [17] [18], arms [19], feet [20] or the head [21]. These researches about vibrotactile perception are usually related to passive perception, but there also are studies focused on determining thresholds for active perception, aiming to improve the realism of perceived patterns or textures through the fingers [22] [23]. Likewise, there are studies to determine force thresholds on fingers [24], both absolute and differential [9].

There are various studies not directly dealing with thresholds or resolution, but related to psychophysical aspects of vibration as well. These studies analyze aspects which might be helpful to create haptic feedback such as the directionality of vibrations [25], absolute perception of haptic patterns [26] [27], or psychophysical aspects inherent to specific haptic devices [10] [28].

Contrarily, the perception over the torso needs to be covered in further detail, even though there already are some references about the resolution [29], as well as the absolute localization both of vibrations [30] [31] and haptic patterns [32]. There are even some studies that state that haptic perception is more accurate and localizable over the torso than over other areas such as forearms or wrists [30] [33]. Notwithstanding, there is a growing build-up of studies about haptic perception to determine, for instance, differential thresholds using coin motors [8], or the vibrotactile spatial acuity with several measurement conditions on the back [34], getting values quite akin to those in the experiment to distribute the actuators over our haptic vest [11].

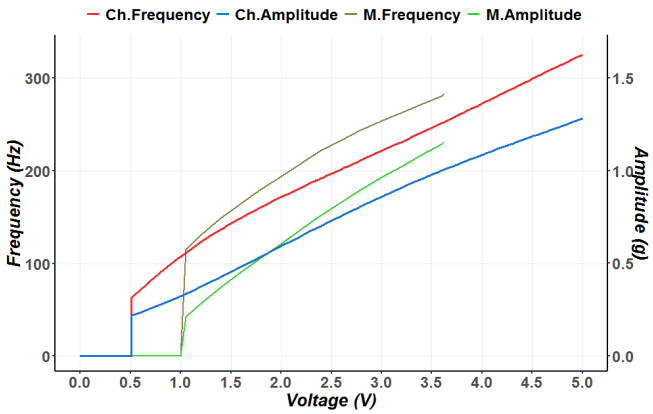

Fig.1. Comparative among the Manufacturer curves (M. Frequency and M. Amplitude) and the curves obtained from the motor's Characterization (Ch. Frequency and Ch. Amplitude).

To conclude, although there is some research about vibrotactile perception, no studies have measured absolute and differential thresholds over the torso using ERM motors. Thus, the main objective of this study is to complete a perception map of the whole torso, including the spatial acuity from the previous research and both absolute and differential vibrotactile thresholds. The values define thorough vibrotactile ranges which could be used to develop reliable haptic patterns with devices containing similar vibrotactile actuators.

III. Experimental Setup

A. Characterization of ERM Motors

The vibrotactile actuators used in this research are cylindrical-shaped ERM motors, whose diameter and length are 5.3 and 20.1 millimeters, respectively (ref. 304-116, Precision Microdrives Limited, London). The operating curve provided by the manufacturer shows that the motors need voltages within the range 1 to 3.6 V to operate. The frequency differs between 120 and 285 Hz, and the vibration amplitude oscillates between 0.2 and 1.3 g (see Fig. 1).

Nevertheless, the experimental conditions are not equal during the data gathering by the manufacturer than if motors are attached to the vest. We then needed to characterize the motors with our particular conditions to establish accurately the frequency and amplitude values that users perceive during a typical operation of the vest.

The characterization is conducted using an Arduino UNO (Arduino, Italy), and a Pulse-Width Modulation (PWM) output, which can take 256 values to power the motor between 0 and 5 V. The system applies the PWM value to a power stage to reach each specific voltage, and the stage also protects the motor against either overcurrent or overvoltage states.

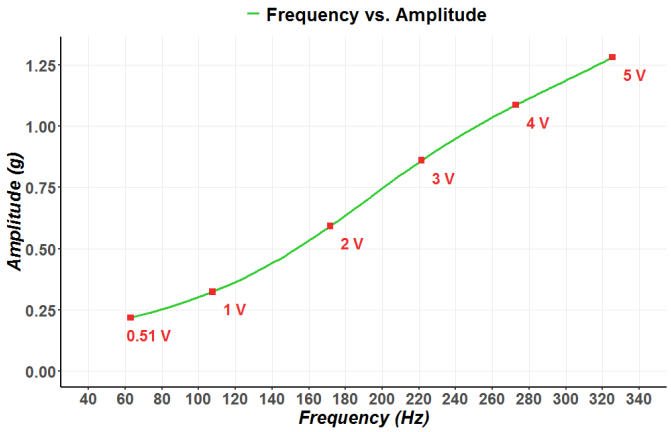

Fig.2. Curve relating the frequency and the amplitude of ERM motors. They begin to vibrate at 0.51 V (i.e. 63 Hz and 0.219 g), and each point of the curve corresponds to a specific supply voltage.

The first step is to obtain the equivalence between each PWM value and the voltage by measuring directly among both motor terminals using a digital multimeter. To obtain the frequency and amplitude curves under our experimental conditions, we increased the voltage from 0 to 5 V in steps of 0.05 V using the PWM-voltage relationship. Each vibration was measured with an omnidirectional microphone (to get the frequency), and an accelerometer (to get the amplitude). The accelerometer also yields frequency values that are compared to the microphone values to reinforce the validity of results.

Both signals were processed, erasing the ambient noise by filtering, and applying a Fourier transform to get the dominant vibration frequency and the amplitude for each voltage. The procedure consisted of 80 measures with three different motors to ensure the reliability of results.

The resulting curves follow similar tendencies to the original ones, but there are slight differences. On the one hand, motors can vibrate at voltages lower than 1 V (0.51 V is the minimum voltage) and, on the other hand, they can operate up to 5 V during prolonged times without malfunction, reaching frequencies and amplitudes beyond the limits given in the datasheet (see Figs. 1 and 2). The frequencies differ between 63 Hz (0.51 V) and 330 Hz (5 V), and amplitudes between 0.25 g (0.51 V) and 1.46 g (5 V).

B. Operating Features of ERM Motors

ERM motors have a noteworthy limitation since we can only modify its voltage to attain specific values of frequency or amplitude (i.e. frequency and amplitude cannot vary separately). Therefore, each vibration depends on a combination of amplitude and frequency [8], and both parameters are valid to characterize the perception of vibrotactile stimuli [35] [36].

Both the datasheet and the characterization curves show relationships roughly linear between voltage, frequency, and amplitude (see Fig. 1). A change of voltage entails proportional variations in frequency and amplitude. We provide two fourth-degree equations to obtain the frequency (F, in Hz) (eq. 1) and the amplitude (A, in g) (eq. 2) for each supply voltage (V) in our experimental conditions. An additional three-degree equation set the relationship between frequency and amplitude (see Fig. 2). All equations are adjusted by polynomial regression based on the characterization data.

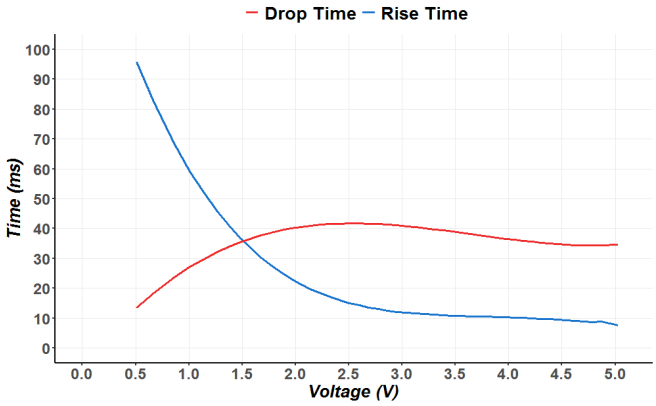

Fig.3. Rise and drop times of the ERM motors in the entire operation range.

$$A = 0.0022V^4 - 0.028V^3 + 0.0114V^2 + 0.085V + 0.15 \quad (1)$$

$$F = -0.657V^4 + 9.204V^3 - 45.99V^2 + 147.5V - 2.5 \quad (2)$$

$$A = -6.72 \cdot 10^{-8}F^3 + 4.1 \cdot 10^{-5}F^2 - 0.0031F + 0.27 \quad (3)$$

Henceforth our results are given in terms of frequency since we consider it eases to carry out comparisons with other vibration motors or the same motors in other experimental conditions. Nevertheless, changes in the perception during the ensuing experiments are not only associated with the frequency but to the whole vibration characterized by particular values of frequency and amplitude. We can obtain the threshold in terms of amplitude by using (3).

Other features of ERM motors that may affect the perception are the rise time (i.e. from the start until the motor reaches 50 % of the vibration amplitude) and the drop time (i.e. from the power interrupts until the motor stops) since values of frequency and amplitude are not accurate during those times. We measured those values in the whole vibratory range of the motors (see Fig. 3). Drop times are practically constant in the entire range. However, rise times are high at low voltages (i.e. low frequencies or amplitudes); thus, stimuli in the first experiment must be long enough (above 100 ms) so that users always perceive the target vibration.

These features differ for different motors, and results are applicable provided that a haptic device contains ERM motors with similar features. If ERM motors have different features, or the actuators can modify the vibratory amplitude and frequency independently, a new calibration would be needed to characterize the vibratory stimuli appropriately.

C. Vest and Motor's Placing

The vest was divided into 16 areas: six areas on the front torso and six on the back, the right lateral, the left lateral, the right shoulder and the left shoulder. Four Velcro strips delimited the areas to place the cloth with the motors during the experiments. The areas and their names appear in Fig. 4.

The wide range of body sizes implied the necessity of tailoring two different vests to ease the wearability (S and L sizes), although the laterals and the shoulders could be adjusted using Velcro strips in order to adapt the vest to the rest of standard sizes (M and XL). The vest was made of neoprene since it is a flexible and readily adjustable material.

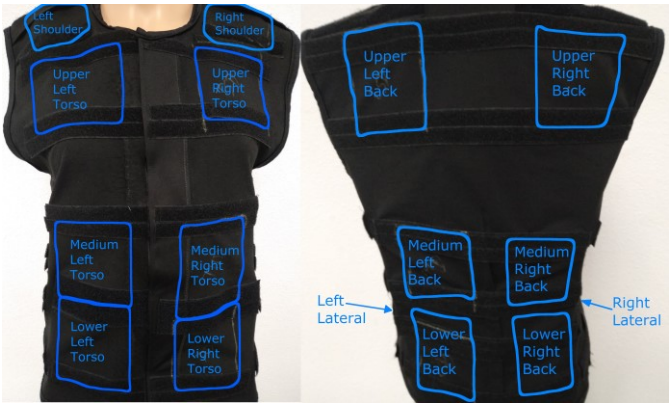

Fig.4. Torso (left) and back (right) side of the vest. The areas are marked with a rectangle and the corresponding names are written inside them.

Three motors were sewn above a cloth made of a rigid fabric to prevent lateral spread of vibrations. The cloth had two Velcro strips to attach it over the 16 areas of the vest in each phase of the experiment (see Fig. 5). The sewing avoids any waste material (e.g. glue) which may affect the vibratory frequency while the motor operates.

The motors are separated 10 millimeters from each other, but the control system always used the same motor to keep conditions unchanged. The motor was always tested before each phase to ensure proper operation, although a change during an experimental phase does not imply perception's variability. The distance between them is lower than our reference of spatial acuity values (around 50 mm) [11], and also lower than values in alternative studies (lower than 20 mm) [37]. Even so, we only had two failures of motors during the whole experiment related to cable breakings.

IV. Absolute Threshold Experiment

A. Apparatus

The experimental system consisted of the driver system to manage the motors as described above for the calibration. The experiments were managed by a Dell Precision 490 Dual-Core Intel Xeon EM64T (graphics card nVIDIA® Quadro® FX 4500, 512 MB) running MATLAB to record the responses (The MathWorks, Inc; Natick, MA) and the Arduino IDE (Arduino, Italy) to handle PWM values and power the motors.

B. Participants

Participants were 22 volunteers, 10 males and 12 females ranging from 21 to 34 years old (mean ± SD, 24.652 ± 3.034 years). They were unaware of the purpose of the study and provided written informed consent. All participants were in-between 18 and 40 years, given that haptic perception changes substantially with aging [38] [39] [40], avoiding troubles to generalize the results. The Ethics Committee of Universidad Politécnica de Madrid approved the experimental procedures, and the study complied with the Code of Ethics of the World Medical Association (Declaration of Helsinki).

Before starting both experiments, participants were asked about diagnosed neurological issues, psychological problems, diseases or medication related to haptic perception [41] [42]. Exclusively participants who had normal haptic perception were selected to take part in the experiment.

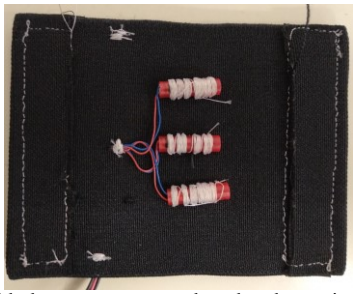

Fig.5. Cloth with three motors, even though only one is used during the experiments. The rest are used in case of malfunctioning or errors.

C. Procedure

The first experiment consisted of measuring the absolute vibration threshold of the 16 areas (see Fig. 4).

For this experiment, we used a two-interval forced-choice (2iFC) task. Each trial was composed of two intervals with a duration of 350 milliseconds by interval and a temporal gap of 1.3 seconds between them. A vibration was randomly assigned to one of the temporal intervals, and no stimulus was presented during the other interval. The participants had to indicate whether the first or the second interval contained the vibratory stimulus by pressing the number 1 or 2 on a numeric keyboard. A new trial started after the participant responded.

All participants performed the experiments with the same type of undershirt which they had to select among different sizes (S, M, L, or XL size). The experimenter then placed the cloth over a specific area, and participants wore the vest afterwards in order to begin the experiment. The vest had to be as tight as possible to ensure proper contact with the skin provided that participants felt utterly comfortable.

A pure tone of 800 Hz was presented before each presentation interval, aiming to indicate the next vibration in order to avoid participant's distraction. Moreover, an intense white noise was presented to mask the sound of vibrations during the presentation interval. The volume of the noise was adjusted before starting the experiment to mask all motor sounds, and to avoid discomfort. Participants heard both the tone and the noise using headphones.

The vibratory frequency of each trial changed according to a Bayesian adaptive staircase [43] [44] [45] whose prior distribution of frequencies was uniform (i.e. non informative about the threshold value), and the model function ($M(x,\theta_i)$) was the Logistic (see [46] and [47]) (the parameters used were guess rate = 0.5, lapse rate = 0.01, delta (δ) = 0.0123, and sigma (σ) = 0.8). We calculate the posterior distribution according to equation (4) in order to update the staircase after the participant's response given in each trial.

$$P_{i+1}(x) = P_i(x)M(x,\theta_i)^C[1-M(x,\theta_i)]^I,\ i \in [1,n] \quad (4)$$

In equation (4): P is the posterior distribution, and M is the model function, C = 1 and I = 0 after a correct response and I = 1 and C = 0 after an incorrect response. The number of trials is n. The mean of the posterior distribution ($\theta_i = \overline{P_i(x)}$) provides the frequency presented in each trial.

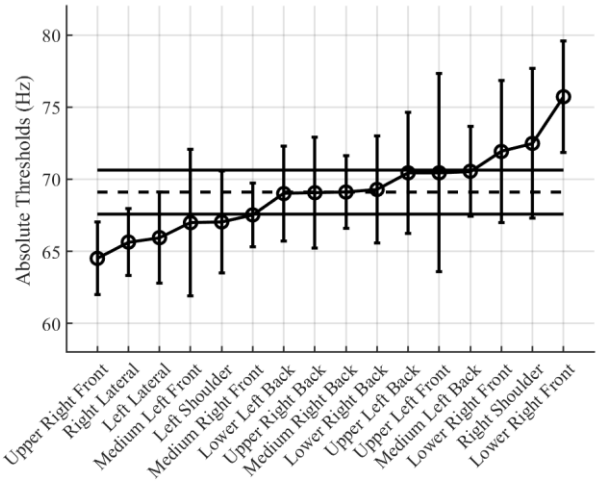

Fig.6. Vibration absolute thresholds for different areas. Each symbol and line represents the mean ± SEM (Standard Error of Mean) of ten subjects per area. The horizontal dashed line corresponds to the mean of vibration absolute thresholds for the sixteen areas (69.1074 Hz) and the horizontal solid lines are the 95% confidence interval of the mean ([67.5802 70.6346] Hz).

The final estimation of the threshold was the mean of the final distribution after completing 40 trials ($P_{n+1}(x), n = 40$). According to this procedure, the absolute threshold is defined as the minimum frequency to detect vibration with a success rate of 75%. Each participant completed three staircases by area to obtain three single measures of the threshold, and the final absolute threshold is the mean of these three measures. Participants had to determine 48 vibrotactile absolute thresholds to complete the experiment.

The total duration to determine all absolute thresholds was 5 hours and 30 minutes per participant. It was an unduly long time to perform the whole experiment without fatigue; hence, there were two options: completing the experiment in several sessions or completing only a part in a single session. The time of the session was between 1 and 2 hours. Each participant completed three areas per hour with a break of 3-5 minutes between areas to avoid fatigue.

Regardless of a participant completed the whole experiment or solely a part; the tested areas were randomized. If haptic perception does not change within the age range between 18 and 40 years old, the distribution of participants per areas could be random without risk of biasing the final results.

The voltage-frequency curve obtained after the calibration must be considered to determine the voltage to apply in every trial. As both experiments used a similar process, an example is illustrated using this experiment: the first frequency displayed by the system could be, for instance, 80 Hz which corresponds to a voltage of 0.71 V, so the driver unit applied a PWM signal of 10% duty cycle. If the user identified the vibration rightly, the driver unit displayed a superior value in the next trial (e.g. 93 Hz, after applying (4)), which corresponds to 0.81 V and a PWM signal of 11% duty cycle. The procedure is similar during the rises and falls of frequency throughout the 40 trials of each experiment.

D. Statistical Analysis

The first experiment estimated the absolute thresholds for sixteen areas. The analysis of the results was performed employing an unequal variance One-Way ANOVA for independent measures (Welch's ANOVA) in order to compare among different areas. Moreover, we used an unequal variance t-test (Welch's t-test) [48] to compare the corresponding parts of the right and left sides of the front torso and back.

TABLE I
COMPARISON BETWEEN RIGHT AND LEFT AREAS

Comparison	t'	p-value
Right Shoulder (RT) vs. Left Shoulder (LT)	1.2230	0.2391
Upper Right Torso (URT) vs. Upper Left Torso (ULT)	1.1486	0.2743
Medium Right Torso (MRT) vs. Medium Left Torso (MLT)	0.1379	0.8926
Lower Right Torso (LRT) vs. Lower Left Torso (LST)	0.8566	0.4036
Upper Right Back (URB) vs. Upper Left Back (ULB)	0.3429	0.7357
Medium Right Back (MRB) vs. Medium Left Back (MLB)	-0.5091	0.6171
Lower Right Back (LRB) vs. Lower Left Back (LLB)	-0.0818	0.9357
Right Lateral (RL) vs. Left Lateral (LL)	-0.1105	0.9133
Right Back vs. Left Back	0.3978	0.6919
Right Torso vs. Left Torso	-0.2208	0.8259
Right Areas vs. Left Areas	0.0893	0.929

Welch's t-test for comparing vibration absolute thresholds of the right and the left areas

E. Results

All thresholds (in Hz) are shown in Fig. 6 as a function of the tested areas. The minimum average value is 64.5103 Hz, which corresponds to the Upper Right Torso (URT), and the maximum average value is 75.7229 Hz, which corresponds to the Lower Right Torso (LRT) (see Fig. 4 for checking up the areas). The average of all absolute thresholds of the sixteen areas was 69.1074 Hz (dashed line in Fig. 6), and the 95% confidence interval of the mean is [67.5802 70.6346] Hz (solid lines in Fig. 6). Despite those differences, Welch's ANOVA shows that there are no significant differences between all absolute vibrotactile thresholds ($F'_{15,54.319} = 1.191,\ p = 0.306$).

Additionally, we have performed several further comparisons: 1) individual areas of right and left side of the front torso and back; 2) all areas of right and left front torso (lateral, upper torso, medium torso, and lower torso); 3) all areas of right and left back (shoulder, right back, medium back, and lower back); 4) all right and all left areas (see Fig. 4 and Table I to check up the areas and the results, respectively). The results of those comparisons do not show any significant difference between areas in the entire torso.

V. Differential Thresholds Experiment

A. Apparatus

The whole experimental system was the same than the system used in the absolute threshold experiment.

B. Participants

Participants were 61 volunteers, 29 males, and 32 females ranging from 18 to 36 years old (mean ± SD, 23.377 ± 4.807 years). The remaining details about participants are the same as those in the absolute threshold experiment.

C. Procedure

This experiment consisted of measuring the differential vibrotactile threshold for three temporal frequencies (reference frequencies): 100, 175 and 225 Hz. We chose these frequencies in order to ascertain if the thresholds follow Weber's law and, in turn, to obtain Weber's fractions for determining the thresholds with whichever reference frequency. The frequencies were selected to encompass the whole range of motors' operation. The first value (100 Hz) is substantially higher than the absolute threshold (69.1 Hz) to ensure the utter perception of all stimuli. The third frequency is the highest possible value to avoid the saturation of the threshold (a phenomenon which might occur if the resulting differential threshold is above the maximum frequency displayable with the motor (330 Hz)). Finally, the second frequency is an intermediate value.

The results of the first experiment did not show significant differences between the absolute thresholds of the right and left sides. Therefore, this experiment was only carried out testing the 8 right areas (see Fig. 4) because we assumed that differential thresholds would be similar in both sides.

We used a vibration matching task where each trial was composed of two temporal intervals with a duration of 350 milliseconds and a temporal gap of one second between presentations. In each interval, one vibration was presented. Each vibration was randomly assigned to the intervals: one contained the reference frequency (100, 175, or 225 Hz), and the other contained the test frequency. The participant's task was to indicate which interval contained the vibration at a higher frequency by pressing the number 1 (the first vibration) or 2 (the second vibration) on a numeric keyboard.

The frequency of the test vibration changed according to a Bayesian adaptive staircase with similar characteristics to the staircase used in the first experiment. The model function ($M(x, \theta_i)$) was the Logistic function (their parameters were guess rate = 0.01, lapse rate = 0.01, delta (δ) = 0.0123, and sigma (σ) = 0.8), and the prior distribution was uniform. The test vibration was also obtained using equation (4), and the mean of the final distribution gives the upper threshold after 40 trials ($P_{n+1}(x), n = 40$). For each staircase, the reference frequency remained fixed on each trial.

The upper differential threshold is defined as the minimum increment of the frequency needed to discriminate the reference and the test vibration with a success rate of 75%. Each participant completed three staircases by area to obtain three upper differential thresholds. The definitive upper threshold of an area was the mean of these three measures. In this case, the procedure was repeated three times to get the results for each reference frequency. Therefore, considering 8 areas, the whole experiment consisted of the measurement of 72 upper differential thresholds (i.e. 24 thresholds per participant and reference frequency).

The total duration to determine all thresholds in 8 areas was 8 hours per participant. As in the first experiment, it was involved to complete all tests without fatigue or distractions. Hence, we use a similar procedure (i.e. several sessions to end the experiment or a single session) with the same duration for each session and the same breaks to reduce fatigue.

There were four shared features between both experiments: 1) the randomization of the tested areas; 2) the usage of a pure tone of 800 Hz to indicate both presentations; 3) the usage of white noise to mask the sound of vibrating motors; 4) the usage of similar undershirts for participants.

The ultimate goal is to settle both upper and lower differential thresholds for each area. We can use the mechanisms of Weber's law and the results of upper thresholds to estimate the lower differential thresholds for whichever reference frequency.

D. Statistical analysis

The second experiment estimated the upper differential thresholds for eight areas of the torso using three reference frequencies (100, 175, or 225 Hz). The analysis of the results was performed employing a One-way ANOVA for independent measures (Welch's ANOVA) with the data of each reference frequency.

E. Results

The upper differential thresholds (in Hz) are shown in Fig. 7 as a function of the eight areas on the right side for three distinct reference frequencies (100, 175, and 225 Hz). The graph shows a clear pattern since the differential thresholds increase with the growth of the reference value; evidencing thresholds are proportional to the intensity of the reference. Hence, the differential thresholds are linear: they are around 10-15 Hz for the first reference frequency (100 Hz); around 25-35 Hz for the second reference (175 Hz), and 45-50 Hz for the third reference (225 Hz).

Welch's ANOVA shows significant differences between the upper differential thresholds of distinct areas when the reference frequency is 100 Hz ($F_{7,31.149} = 2.91,\ p = 0.018$). Therefore, the differences between areas must be analyzed using a posthoc Tukey test, revealing there are significant differences between the Upper Right Torso (URT) and several areas which Table II reports. Nevertheless, the results of Welch's ANOVA when the reference frequencies are 175 Hz ($F_{7,30.73} = 1.037,\ p = 0.426$) and 225 Hz ($F_{7,30.79} = 0.622,\ p = 0.733$) do not show significant differences among areas.

The proportionality of the thresholds and the reference frequencies are associated with Weber's law, which proposes that the ratio between the upper differential threshold (ΔF) and the reference frequency (F) is a constant value (K) known as

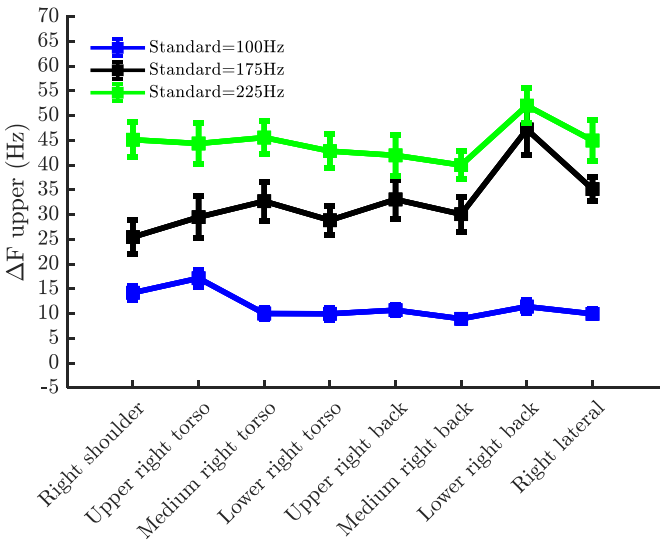

Fig.7. Upper difference thresholds (ΔF_{up}) for the eight areas tested and three standard temporal frequencies. Each symbol and line represents the mean ± SEM (Standard Error of Mean).

TABLE II
SIGNIFICANT RESULTS OF TUKEY TEST FOR DIFFERENTIAL THRESHOLDS

Comparison	Difference	SEM	p-value
URT vs. MRT	7.128	1.938	0.01
URT vs. LRT	7.053	1.938	0.011
URT vs. URB	6.444	1.894	0.023
URT vs. MRB	8.186	1.894	0.001
MRT vs. RL	7.193	1.938	0.009

Tukey Post-hoc Test for analyzing the differences between areas based on the significant difference generated by the One-way ANOVA

Weber fraction ($K = \Delta F/F$). Thereby, the results of all measured thresholds (see Fig. 7) afford to determine Weber fraction for each area and reference frequency (see Fig. 8).

The objective is to get a single Weber fraction which embraces the three individual fractions corresponding to the three references in a single area. The three K-values were adjusted into a line using a linear least-squares fitting, obtaining a general fraction for each vest's area. In such a manner, the resulting Weber fraction of each area (i.e. K, the slope of the fitted line) serves to attain the theoretical lower and upper differential thresholds using the Weber function ($\Delta F = K \times F$). The obtained fittings for each area appear in Fig. 9, besides the estimated Weber fraction (K) on the top-left part of each panel. Additionally, Table III reports the estimated K-values and the coefficient of determination (R^2).

The estimated K-values for each analyzed area are reported in Fig. 10. The graph shows a striking result since an area remarkably differs from the rest (Lower Right Back (LRB) has a K-value of 0.231, whereas the remaining areas have K-values between 0.17 and 0.19). Moreover, the sensitivity of the system yields the same results (see Fig. 11), owing to it is the reciprocal of Weber fraction ($S = 1/K$), and, hence, both values are proportional.

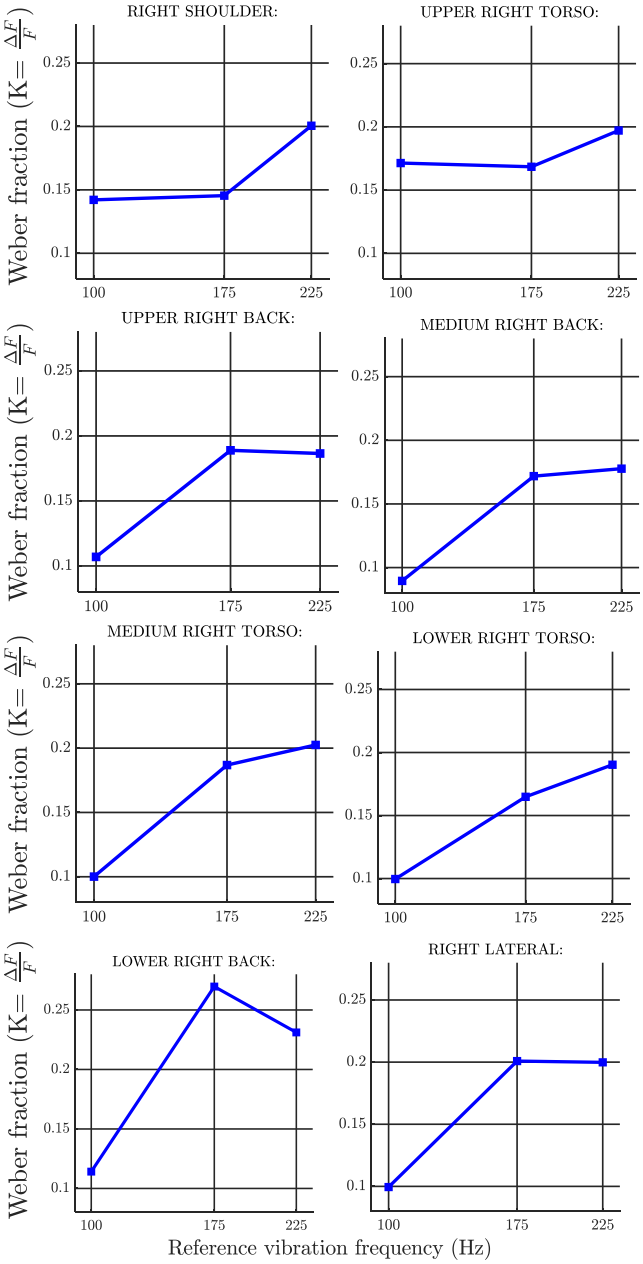

Fig.8. Weber fraction (K) as a function of the reference frequency from data presented in Fig. 7. Each panel corresponds to an area tested.

The fitted K-values might be used to predict roughly whichever upper differential threshold for any reference frequency. The procedure consists in selecting a reference frequency and an area and predicting the differential threshold using Weber function ($\Delta F = K \times F$). The prediction of upper differential thresholds is shown in Fig. 12 (solid lines), using the K-values from Fig. 9.

The second objective was to determine the lower differential thresholds. Weber's law provides a method to obtain the value of lower differential thresholds for any reference frequency using the equation $\Delta F = (K \times F)/(1 + K)$. The predictions (dashed lines) for the three references of the experiment are shown in Fig. 12, and the K-value of each area is taken from Table III.

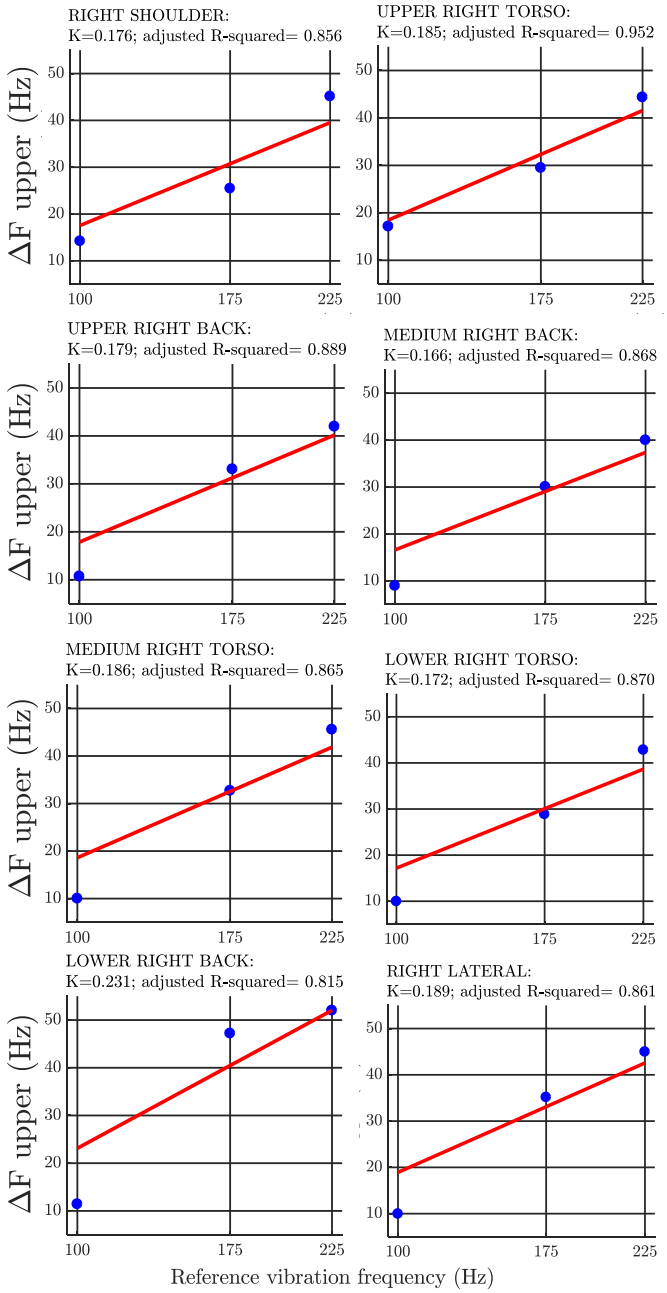

Fig.9. Weber fraction (K) estimated from the data shown in Fig. 7 for different areas. The fitted value (K) and coefficient of determination (R^2) are represented in the top-left part of each panel.

VI. DISCUSSION

Both psychophysical experiments serve to estimate the absolute and differential thresholds of several regions of the torso. The aim is to establish a psychophysical basis for creating haptic patterns using ERM motors. Both thresholds allow to create patterns which users always perceive (all stimuli must be more intense than the absolute threshold), but further, they must readily perceive each successive stimuli by using the differential thresholds and Weber's law during the creative procedure. All results (absolute thresholds and K-values of differential thresholds) are reported in Fig. 13 for each area of the vest. As we mentioned before, the perception depends on particular values of frequency and amplitude [8].

TABLE III
RESULTS OF FITTINGS – WEBER'S LAW

Area	Weber Fraction ($K = \frac{\Delta F}{F}$)	Adjusted R^2
Right Shoulder	0.176	0.856
Upper Right Torso	0.185	0.952
Upper Right Back	0.179	0.889
Medium Right Back	0.166	0.868
Medium Right Torso	0.186	0.865
Lower Right Torso	0.172	0.870
Lower Right Back	0.231	0.815
Right Lateral	0.189	0.861

Values of the Weber Fraction (K) estimated by fitting the data presented in the Fig. 7. The values of K and the coefficient of determination (R^2) are taken from the Fig. 9.

We also use the frequency all through the discussion, but each stimulus is also characterized by the amplitude that we can obtain using (3).

Comparing our results with prior studies is certainly complex since no many investigations have examined these thresholds over the torso (most of the research has their focus on other body regions [29] [35]). Previous studies over the torso seek to determine other aspects such as the spatial acuity [8] [29] or the absolute localization [30] [31]. Even so, the usage of our estimated thresholds alongside those studies is beneficial to enhance the creation of haptic patterns.

A. Experiment 1. Absolute Thresholds.

The main finding of this experiment is the similarity of vibrotactile absolute thresholds in all tested regions of the torso: the differences between areas of the vest, and between the left and right sides of the body are not significant. Thereupon, we set the absolute threshold as the average value of all tested regions (69.1074 Hz, SEM = 0.7165), which remains constant in the front torso and back.

As a result, all stimuli of a haptic pattern must generate a vibration of frequencies above this absolute threshold, regardless of the vest's area wherein the pattern is displayed. The adequate option to ensure the perception of whichever haptic sequence is to set a superior value to the average (e.g. 80 Hz), in order to guarantee a broad leeway to create perceivable patterns in the entire torso for all users.

Despite the lack of significant differences among areas, Fig. 6 shows differences of up to 10-11 Hz (e.g. URT vs LRT) which may look like two discernible stimuli. However, the results of the second experiment endorse the statistical analysis and show that this difference is not significant (i.e. both stimuli would seem identical to users). For instance, we can estimate the upper differential threshold for the average value of the absolute threshold (69.1074 Hz) using the K-values in order to verify if the predicted differential threshold is superior to the maximum difference among areas. Thereby, we estimate the differential threshold with the lower K-value (see Table III), obtaining an estimation of 11.62 Hz ($\Delta F = 69.1074 \times 0.166 = 11.62\ Hz$) that is higher than the difference between the maximum and the minimum absolute thresholds (i.e. $75.7229 - 64.5103 = 11.21\ Hz$).

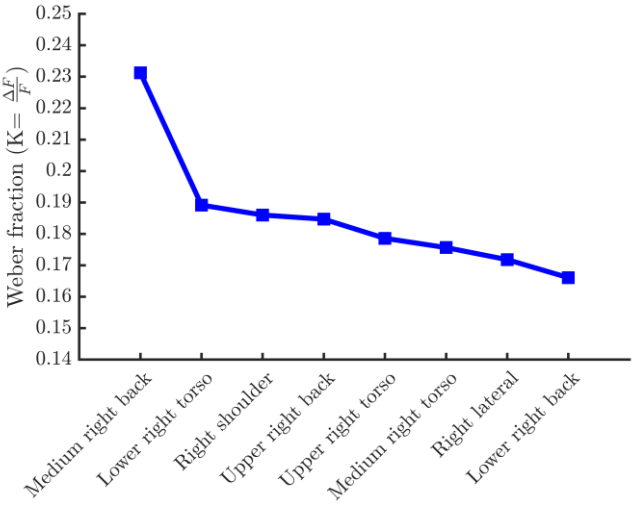

Fig.10. Weber fractions (see Table III) for different areas.

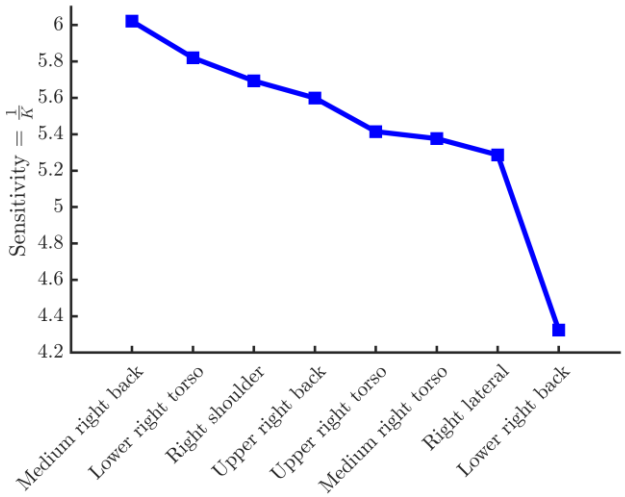

Fig.11. Sensitivity for different areas (see Fig. 4). Sensitivity was estimated as the reciprocal of Weber fraction using the K-values from Table 2. Note that areas are ordered from highest (left) to lowest (right) sensitivity.

B. Experiment 2. Differential Thresholds

The results show the proportional relation between the differential thresholds and the reference frequencies, which agrees with the results of previous experiments over other areas of the body [49]. The increase of the reference frequency entails, in turn, an increase of the average value of the differential threshold (see Figs. 7 and 12). In this manner, if users perceive a 100 Hz vibration, they will need an increase of approximately 10-15 Hz to discriminate the stimulus; whereas if the first stimulus is a 225 Hz vibration, they will discriminate the next stimulus if the change is about 40-50 Hz.

On the other hand, our results show that there are no significant differences between differential thresholds when the reference frequencies are 175 and 225 Hz; however, there is a particular area (Upper Right Torso) which shows significant differences concerning other five regions when the reference frequency is 100 Hz (see Fig. 9).

This fact is rather exceptional, and its causes are hardly inferable. We discarded hardware troubles since the analysis of every staircase does not show plain deviations. Another

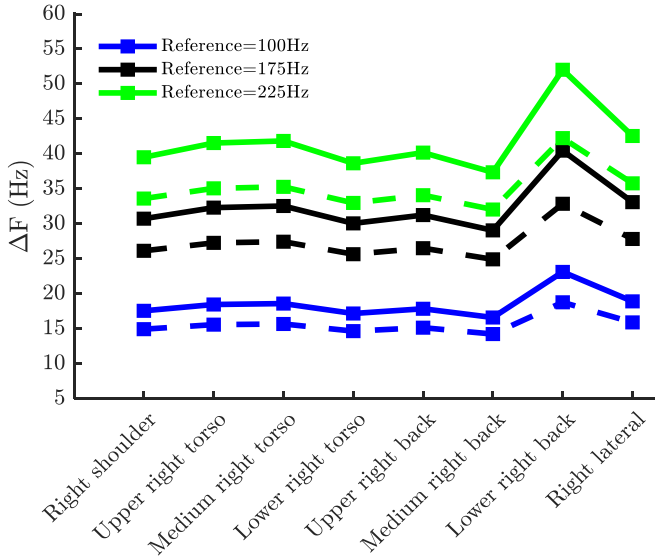

Fig.12. Predicted differential thresholds (ΔF) for different areas using the estimated values of K from Fig. 9. Solid lines represent the upper difference threshold and dashed lines represent the lower difference threshold.

option is the lack of attention due to stress or fatigue, but users knew they may stop the experiment if they needed a break or were not comfortable. Nevertheless, the fitting of the vest over the skin is a likely cause since it can change the contact surface of motors, and results might differ [37]. Even so, the adjustment and pressure of motors over the skin were verified before starting each phase to minimize troubles. Another possibility is that the difference might be caused by the motors pressing osseous or soft areas; however, this cannot be the reason given that the location of actuators was thoroughly examined to avoid placing them over bone tissue, even though bodies vary as regards size and shape.

Our results indicate that differential thresholds follow Weber's law. We have estimated Weber fractions (K) for each separate area, obtaining K-values that oscillate between 0.17 and 0.19, which are values rather akin to others from previous studies over fingers or forearm [36] [50]. The LRB area has a value of 0.231 (Figs. 7 and 8 reveal a value following a different tendency in that area) which is notably different to the rest of areas (as the sensitivity plot also shows in Fig. 11).

This difference indicates that, under certain conditions, the thresholds might vary, but those differences are not conclusive since the variations occur in a particular case that is not enough to be generalized. In the light of the results, we can conclude that differential thresholds are similar across the vest's areas, and therefore we could use a single K-value to create haptic patterns in a generalized way for the entire vest.

Lower differential thresholds are also based on K-values and reference frequencies, and predictions have the same pattern as the upper thresholds (see Fig. 12). Note that according to Weber's law, lower thresholds require a smaller difference (e.g. for a reference of 225 Hz, the upper threshold is around 40 Hz, and the lower threshold is around 35 Hz).

Therefore, selecting a K-value (e.g. K = 0.2) and a reference frequency (e.g. 100 Hz), it is possible to determine the upper and lower frequency that a user can discriminate according to Weber's law. For instance, if the first phase of a pattern is a stimulus of 100 Hz, users can solely discriminate a vibration

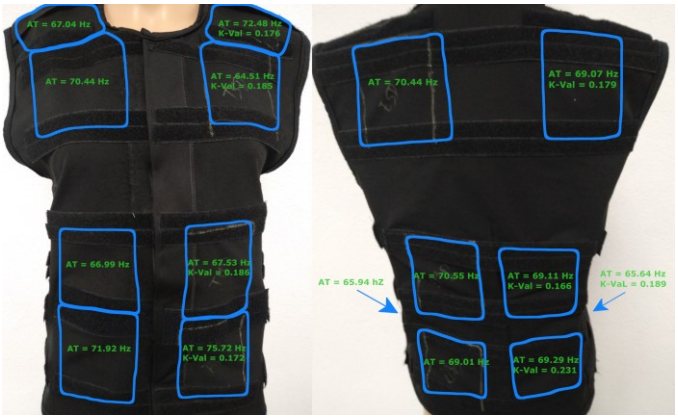

Fig.13. Results of absolute threshold (AT) across the areas (at Hz) and K-value (KVal) of Weber's law of the differential thresholds on right areas

of 120 Hz ($100 + 100 \times 0.2 = 120$) as a distinct stimulus from the pattern (note that if we used the estimated K-value, the vibrations would be discriminable with a success rate of 75%, according to the followed procedure).

In summary, results of both thresholds are similar among areas, and it is viable to create haptic patterns using constant values given that users evenly perceive stimuli over the entire torso. In this manner, a pattern composed of three successive vibrotactile stimuli would have some requisites. The three stimuli must vibrate with frequencies above the absolute threshold (e.g. 80 Hz or superior). Moreover each successive stimulus must fulfill the differential threshold estimated with Weber's law. To this end, the K-value must be slightly superior to the experimental ones (e.g. K = 0.2), and if the first vibration is of 100 Hz, the next one must be of 120 Hz or higher to ensure the perception of both stimuli.

C. *Additional Considerations*

The distribution of mechanoreceptors over the torso is a leading aspect to comprehend the results. Pacinian corpuscles are the main involved in the perception over the torso since they detect vibrotactile stimuli between 40 and 600 Hz, approximately (i.e. a range which includes the entire vibratory range of motors). Moreover, they are distributed widely over the front torso and the back [50], which might clearly explain the resemblance of results. Other receptors might also condition the perception, but their influence is negligible. Hair receptors in the torso perceive vibrations as well, but their distribution is not uniform and it hinges on the body area or the gender (male or female). Moreover, they only become activated with low-frequency vibrations and high amplitudes (20-50 Hz) that this motor does not reach. Ruffini cylinders are only in the hands, and the Meissner corpuscles can solely detect low-frequency contacts (10-50 Hz) [50] [51] [52] [53].

Rise and drop times of ERM motors may affect the perception of vibrotactile stimuli. However, vibrations only activate Pacinian corpuscles during those times since the remaining receptors do not respond to frequencies lower than minimum frequency of this motor (i.e. 63 Hz). Thus, obtained results are reliable because each stimulus always reached the target frequency (i.e. durations were longer than 100 ms).

Both the absolute and differential vibrotactile thresholds have been obtained using an ERM motor with specific features (frequency, amplitude or voltages). However, other haptic devices may use different actuators (e.g. coin motors or LRAs), which further can offer control over the amplitude separately, providing more possibilities to create patterns. Therefore, the results of these studies may be applied provided that the features of actuators are similar to the ERM motors used in this paper [37]. Otherwise, it would be needed to repeat the experiments in order to ascertain the similarities and the applicability of these results to create haptic patterns with other vibrotactile actuators [37].

Results serve to establish a guideline for creating haptic patterns with a vest which includes ERM motors. Not only do these thresholds and the spatial acuity need to be considered, but other phenomena can strengthen the creation of haptic feedback. There exist aspects directly related to the creation such as the directionality of vibrations or the spans between successive stimuli, whose adjustment can enhance the conveyance of information [3] [54]. Furthermore, the orientation of motors (vertical or horizontal) may also be relevant. It would be suitable to conduct additional research to ascertain how to use those aspects and how they affect the spatial acuity or the thresholds (either absolute or differential).

Likewise, there are some outstanding psychophysical phenomena such as the spatial summation, although a proper distribution of motors according to the spatial acuity should minimize or remove its influence [12]. Moreover, users can undergo either adaption or masking, which dynamically changes the thresholds [13] [14]; thus, the patterns must be adjusted by continuously altering the sequence or using offset times to prevent these effects [8] [25].

Our results can vastly simplify subsequent studies since they show the uniformity of vibrotactile perception in the torso. Additional experiments could be conducted over some specific areas since results would also be generalizable, either to extend the knowledge of these ERM motors or to ascertain psychophysical values with other actuators.

VII. Conclusions

This paper proposes the characterization of the vibrotactile perception over the entire torso by defining some distinctive parameters using a vibration ERM motor. Thereby, haptic patterns can be created based on reliable empirical results to render them by using a haptic vest containing these particular motors. Those patterns can convey accurate information to users via a haptic vest (either through intricate patterns coming from a virtual scenario, navigation cues, or other means). The vibrotactile spatial acuity, the absolute and the differential vibrotactile thresholds are the most relevant parameters to create patterns adequately. There are plenty of studies about spatial acuity, but both absolute and differential thresholds are mostly unexplored. Our results shed light over these unknown but crucial aspects to develop dependable vibrotactile patterns.

Results of the first experiment show that the estimation of absolute thresholds is almost constant in the entire torso, which is the first step to generalize the creation of haptic patterns. It is then feasible to set a value which serves as a reference to create vibrotactile stimuli. That value must be superior to the empirical average threshold (i.e. 64.8 Hz) to ensure every stimulus is always perceivable in the front torso or the back (e.g. 80 Hz or above).

The estimation of differential thresholds from the second experiment shows the same trend. We measured differential vibrotactile thresholds for three reference frequencies in order to obtain Weber fractions (i.e. K-values). Those values are similar in the entire torso, even though there is a significant difference which is disposable since it only appears in a particular case. We can then set the same K-value to estimate any differential threshold according to Weber's law. Moreover, that K-value allows an easy estimation both the upper and lower differential thresholds throughout the vibratory range of these motors.

It is not advisable to adopt these particular values without verifying the motors' features in advance due to values can substantially change. However, this procedure may be valid to obtain those values for whichever motor regardless of their features. Moreover, these results also evince the perception is similar in the entire torso, and we can create haptic patterns in a generalized way, which are easily discriminable, detectable, and relatable to specific instructions from human-machine systems that include analogous haptic devices.

ACKNOWLEDGMENTS

We want to thank Raúl Luna del Valle for reviewing the English writing. This study was supported by PGC2018-093406-B-I00 from Ministerio de Economía y Competitividad (Secretaría de Estado de Investigación, Desarrollo e Innovación), Spain to ISP (http://www.mineco.gob.es). SAP is supported by the fellowship Jae Intro 2016 JAEINT_16_00039 from Ministerio de Economía y Competitividad and Consejo Superior de Investigaciones Científicas (CSIC). The funders had no role in the study design, the data collection and analysis, the decision to publish, or the preparation of the manuscript.

REFERENCES

[1] D. Prattichizzo, F. Chinello, C. Pacchierotti, and M. Malvezzi, "Towards Wearability in Fingertip Haptics: a 3-DoF Wearable Device for Cutaneous Force Feedback", *IEEE Trans. Haptics*, Vol. 6, No. 4, pp. 506-516, 2013.

[2] S. Choi and K.J. Kuchenbecker, "Vibrotactile Display: Perception, Technology and Applications", *Proc. IEEE*, Vol. 101, No. 9, pp. 2093-2104, 2013.

[3] A. Cosgun, E.A. Sisbot, and H.I. Christensen, "Evaluation of Rotational and Directional Vibration Patterns on a Tactile Belt for Guiding Visually Impaired People", *IEEE 2014 Haptics Symp. (HAPTICS)*, pp. 367-370, 2014.

[4] G. García-Valle, M. Ferre, J. Breñosa and D. Vargas, "Evaluation of Presence in Virtual Environments: Haptic Vest and User's Haptic Skills", *IEEE Access*, Vol. 6, pp. 7224-7233, 2018.

[5] K.J. Kuchenbecker, J. Romano and W. McMahan, "Haptography: Capturing and Recreating the Rich Feel of Real Surfaces", *Robot. Res.*, pp. 245-260, 2011, Springer, Berlin, Heidelberg.

[6] L.A. Jones and H.Z. Tan, "Application of Psychophysical Techniques to Haptic Research", *IEEE Trans. Haptics*, Vol. 6, No. 3, pp. 268-284, 2013.

[7] S. Dosen, A. Ninu, Y. Yakimovich, H. Dietl, and D. Farina, "A Novel Method to Generate Amplitude-Frequency Modulated Vibrotactile Stimulation", *IEEE Trans. Haptics*, Vol. 9, No. 1, pp. 3-12, 2015.

[8] H.C. Stronks, D.J. Parker and N.Barnes, "Vibrotactile Spatial Acuity and Intensity Discrimination on the Lower Back using Coin Motors", *IEEE Trans. Haptics*, Vol. 9, No. 4, pp. 446-454, 2016.

[9] C. Hatzfeld, S. Cao, M. Kupnik and R. Werthschützsky, "Vibrotactile Force Perception – Absolute and Differential Thresholds and External Influences", *IEEE Trans. Haptics*, Vol. 9, No. 4, pp. 586-597, 2016.

[10] X. Guo, Y. Zhang, D. Wang and J. Jiao, "Absolute and Discrimination Thresholds of a Flexible Texture Display", *IEEE World Haptics Conf. (WHC)*, pp. 269-274, June 2017.

[11] G. García-Valle, M. Ferre, J. Breñosa, R. Aracil, J.M. Sebastián and C. Giachritsis, "Design and Development of a Multimodal Vest for Virtual Immersion and Guidance", *Int. Conf. on Human Haptic Sensing and Touch Enabled Comput. Appl.*, pp. 251-262, July 2016. Springer, Cham.

[12] R.T. Verrillo and G.A. Gescheider, "Enhancement and Summation in the Perception of Two Successive Stimuli"", *Perception & Psychophysics*, Vol. 18, No. 2, pp. 128-136, 1975.

[13] J.C. Craig and P.M. Evans, "Vibrotactile Masking and the Persistence of Tactual Features", *Perception & Psychophysics*, Vol. 42 No. 4, pp. 309-317, 1987.

[14] R.T. Verrillo, "Effect of Contactor Area on the Vibrotactile Threshold", *The Journal of the Acoustical Society of America*, Vol. 35, No. 12, pp. 1962-1966, 1963.

[15] C. Hatzfeld, S. Dorsch, C. Neupert and M. Kupnik, "Influence of Surgical Gloves on Haptic Perception Thresholds", *The Int. J. of Med. Robot. and Comput. Assisted Surgery*, Vol. 14, No. 1, e1852, 2018.

[16] A.J. Doxon, D.E. Johnson, H.Z. Tan and W.R. Provancher, "Human Detection and Discrimination of Tactile Repeatibility, Mechanical Backlash, and Temporal Delay in a Combined Tactile-Kinesthetic Haptic Display System", *IEEE Trans. Haptics*, Vol. 6, No. 4, pp. 453-463, 2013.

[17] L. Scalera, S. Seriani, P. Gallina, M. Di Luca and A. Gasparetto, "An Experimental Setup to Test Dual-Joystick Directional Responses to Vibrotactile Stimuli", *IEEE Trans. Haptics*, 2018.

[18] C. Salisbury, R.B. Gillespie, H. Tan, F. Barbagli and J.K. Salisbury, "Effects of Haptic Device Attributes on Vibration Detection Thresholds", *3rd Joint EuroHaptics Conf. and IEEE Symp. on Haptic Interfaces for Virtual Environments and Teleoperator System, WorldHaptics 2009*, pp. 115-120, Mar. 2009.

[19] T. Miyaoka and T. Nakamura, "Measurements of Detection Thresholds Presenting Normal and Tangential Vibrations on Human Hairy Skin", *Proc. of Fechner Day*, Vol. 22, No. 1, pp. 229-232, 2006.

[20] G.A. Gescheider, S.J. Bolanowski Jr, R.T. Verrillo, D.J. Arpajian and T.F. Ryan, "Vibrotactile Intensity Discrimination Measured by Three Methods" , *The Journal of the Acoustical Society of America*, Vol. 87, No. 1, pp. 330-338, 1990.

[21] V.A. de Jesus Oliveira, L. Nedel, A. Maciel, and L. Brayda, "Spatial Discrimination of Vibrotactile Stimuli around the Head", *2016 IEEE Haptic Symp. (HAPTICS)*, pp. 1-6, Apr., 2016. IEEE.

[22] S.A. Cholewiak, K. Kim, H.Z. Tan and B.D. Adelstein, "A Frequency-Domain Analysis of Haptic Gratings", *IEEE Trans. Haptics*, Vol. 3, No. 1, pp. 3-14, 2010.

[23] S. Papetti, H. Järveläinen, B.L. Giordano, S. Schiesser and M. Fröhlich, "Vibrotactile Sensitivity in Active Touch: Effect of Pressing Force", *IEEE Trans. Haptics*, Vol. 10, No.1, pp. 113-122, 2017.

[24] H.H. King, R. Donlin and B. Hannaford, "Perceptual Thresholds for Single vs. Multi-Finger Haptic Interaction", *IEEE Haptics Symp. 2010*, pp. 95-99, IEEE, Mar. 2010.

[25] M. Eid, G. Korres and C.B.F. Jensen, "SOA Thresholds for the Perception of Discrete/Continuous Tactile Stimulation", IEEE *7th Int. Workshop on Quality of Multimedia Experience (QoMEX)*, May 2015.

[26] D. Wang, C. Peng, N. Afzal, W. Li, D. Wu and Y. Zhang, "Localization Performance of Multiple Vibrotactile Cues on Both Arms", *IEEE Trans. Haptics*, Vol. 11, No. 1, pp. 97-106, 2018.

[27] R.W. Cholewiak and A.A. Collins, "Vibrotactile Localization on the Arm: Effects of Place, Space, and Age", *Perception & Psychophysics*, Vol. 65, No.7, pp. 1058-1077, 2003.

[28] I. Oakley, Y. Kim, J. Lee and J. Ryu, "Determining the Feasibility of Forearm Mounted Vibrotactile Displays", *14th Symp. on Haptic Interfaces for Virtual Environment and Teleoperator Systems*, 2006, pp. 27-34.

[29] J.B. Van Erp, "Vibrotactile Spatial Acuity on the Torso: Effects of Location and Timing Parameters", *1st Joint Eurohaptics Conf. and Symp. on Haptic Interfaces for Virtual Environment and Teleoperator Systems: WorldHaptics 2005*, pp. 80-85, Mar. 2005.

[30] L.A. Jones and K. Ray, "Localization and Pattern Recognition with Tactile Displays", *Symp. on Haptic Interfaces for Virtual Environment and Teleoperator Systems, 2008*, pp. 33-39, Reno, 2008.

[31] R.W. Cholewiak, J.C. Brill and A. Schwab, "Vibrotactile Localization on the Abdomen: Effects of Place and Space", *Perception & Psychophysics*, Vol. 66, No. 6, pp. 970-987, 2004.

[32] J.B. Van Erp, "*A*bsolute Localization of Vibrotactile Stimuli on the Torso", *Perception & Psychophysics*, Vol. 70, No. 6, pp. 1016-1023.
[33] E. Piateski and L. Jones, "Vibrotactile Pattern Recognition on the Arm and Torso", *1st Joint Eurohaptics Conf. and Symp. on Haptic Interfaces for Virtual Environment and Teleoperator Systems: WorldHaptics 2005*, pp. 90-95, IEEE, Mar. 2005.
[34] O.I. Jóhanesson, R. Hoffmann, V.V. Valgeirsdóttir, R. Unnbórsson and A. Moldoveanu, "Relative Vibrotactile Spatial Acuity of the Torso", *Exp. Brain Research*, Vol. 235, No. 11, pp. 3505-3515, Nov. 2017.
[35] H. Pongrac, "Vibrotactile Perception: Examining the Coding of Vibrations and the Just Noticeable Difference Under Various Conditions", *Multimedia Systems*, Vol. 13, No. 4, pp. 297-307, 2008.
[36] A. Israr, H.Z. Tan, and C.M. Reed, "Frequency and Amplitude Discrimination along the Kinesthetic-Cutaneous Continuum in the Presence of Masking Stimuli", *The Journal of the Acoustical Society of America*, Vol. 120, No. 5, pp. 2789-2800, 2006.
[37] R. Hoffmann, V.V. Valgeirsdóttir, Ó. I. Jóhannesson, R Unnthorsson, and Á. Kristjánsson, "Measuring Relative Vibrotactile Spatial Acuity: Effects of Tactor Type, Anchor Points and Tactile Anisotropy", *Exp. Brain Research*, Vol. 236, No. 12, pp. 3405-3416, 2018.
[38] E. Amaied, R. Vargiolu, J.M. Bergheau and H. Zahouani, "Aging Effect on Tactile Perception: Experimental and Modelling Studies", *Wear*, No. 332, pp. 715-724, 2015.
[39] M. Valeriani, F. Ranghi and S. Giaquinto, "The Effects of Aging on Selective Attention to Touch: A Reduced Inhibitory Control in Elderly Subjects", *Int. J. of Psychophysiology*, No. 49, Vol. 1, pp. 75-87, 2003.
[40] E. Poliakoff, S. Ashworth, C. Lowe and C. Spence., "Vision and Touch in Ageing: Crossmodal Selective Attention and Visuotactile Spatial Interactions", *Neuropsychology*, No. 44, Vol. 4, pp. 507-517, 2006.
[41] M. Grunwald, C. Ettrich, W. Krause, B. Assmann, A. Dhne, T. Weiss and H.J. Gertz., "Haptic Perception in Anorexia Nervosa Before and After Weight Gain", *Journal of Clinical and Experimental Neuropsychology*, No. 23, Vo. 4, pp. 520-529, 2001.
[42] J. Konczak, A. Sciutti, L. Avanzino, V. Squeri, M. Gori, L. Masia, G. Abbruzzese and G. Sandini, "Parkinson's Disease Accelerates Age-Related Decline in Haptic Perception by Altering Somatosensory Integration", *Brain*, No. 135, Vol. 11, pp. 3371-3379, 2012.
[43] P.E. King-Smith, S.S. Grigsby, A.J. Vingrys, S.C. Benes, and A. Supowit, "Efficient and Unbiased Modifications of the QUEST Threshold Method: Theory, Simulations, Experimental Evaluation and Practical Implementation", *Vision Research*, Vol. 34, No. 7, pp. 885-912, 1994.
[44] B. Treutwein, "Adaptive Psychophysical Procedures", *Vision Research*, Vol. 35, No. 17, pp. 2503-2522, 1995.
[45] I. Serrano-Pedraza, M.J. Gamonoso-Cruz, V. Sierra-Vázquez, and A.M. Derrington, "Comparing the Effect of the Interaction Between Fine and Coarse Scales and Surround Suppression on Motion Discrimination", *Journal of Vision*, Vol. 13, No. 11, pp. 5-5, 2013.
[46] I. Serrano-Pedraza, W. Herbert, L. Villa-Laso, M. Widdall, K. Vancleef, and J.C.A. Read, "The Stereoscopic Anisotropy Develops During Childhood", *Investigative Ophthalmology & Visual Science*, Vol. 57, No. 3, pp. 960-970, 2016.
[47] P.L. Emerson, "Observations on Maximum-Likelihood and Bayesian Methods of Forced-Choice Sequential Threshold Estimation", *Perception & Psychophysics*, Vol. 39, pp. 151-153, 1986.
[48] G.D. Ruxton, "The Unequal Variance T-Test is an Underused Alternative to Student's T-Test and the Mann-Whitney U Test", *Behavioral Ecology*, Vol. 17, No. 4, pp. 688-690, 2006.
[49] R.T. Verrillo and A.J. Capraro, "Effect of Stimulus Frequency on Subjective Vibrotactile Magnitude Functions", *Perception & Psychophysics*, Vol. 17, No.1, pp. 91-96, 1975.
[50] D.A. Mahns, N.M. Perkins, V. Sahai, L. Robinson, and M.J. Rowe, "Vibrotactile Frequency Discrimination in Human Hairy Skin, *Journal of Neurophysiology*, Vol. 95, No. 3, pp. 1442-1450, 2006.
[51] L. Costanzo, "Physiology", *ElSevier*, 6th Edition, 2017.
[52] F. McGlone, and D. Reilly, "The Cutaneous Sensory System", *Neuroscience & Biobehavioral Reviews*, Vol. 34, No. 2, pp. 148-159, 2010.
[53] S. Gilman, "Joint Position Sense and Vibration Sense: Anatomical Organisation and Assessment", *Neurosurgery & Psychiatry*, Vol. 73, No. 5, pp. 473-477
[54] S.D. Novich, and D.M. Eagleman, "Using Space and Time to Encode Vibrotactile Information: Toward an Estimate of the Skin's Achievable Throughput", *Exp. Brain Research*, Vol. 233, No. 10, pp. 2777-2788, 2015.

Gonzalo García-Valle received his B.S. in Electronics and Automation Engineering in 2014 and M.S. in Automation and Robotics in 2016 from Universidad Politécnica de Madrid (UPM). He is currently a PhD candidate in Automation and Robotics in UPM. Since 2015, he has been a Researcher at the Centre for Automation and Robotics – CAR (UPM-CSIC). His research interests include haptic devices and wearables applied to the human body, thermal and vibrotactile displays, development of haptic actuators, perception, psychophysics and, presence and realism of virtual environments.

Sandra Arranz-Paraíso received her B.S. in Psychology, granted with Grade Extraordinary Prize, in 2016 and M.S. in Methodology in 2018 from Complutense University of Madrid (UCM). Currently, she is a PhD candidate (supported with FPU16/02683 from Ministerio de Educación, Spain) in Experimental and Applied Psychology studying the inhibitory mechanisms that underlie visual motion perception. She has been a Researcher at the Centre for Automation and Robotics – CAR (UPM-CSIC) in 2016. Her research interests include haptic and visual perception, psychophysics, presence and realism of virtual environments, methods and statistics.

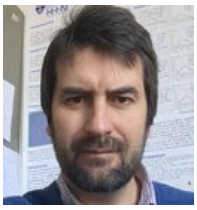

Dr Ignacio Serrano-Pedraza is Profesor Titular at Department of Experimental Psychology (Complutense University of Madrid) since 2010. He completed his PhD in Experimental and Applied Psychology studying second-order visual mechanisms at Complutense University of Madrid in 2005. He is the Director of the Laboratory of Visual Psychophysics at Complutense University of Madrid. His lab works on different aspects of visual perception, like stereoscopic or 3D vision, spatial vision, and motion perception. More information about his projects and publications can be found at the Laboratory webpage: https://www.ucm.es/serranopedrazalab.

Prof. Manuel Ferre received the Laurea Degree in Control Engineering and Electronics in 1992 and PhD in Automation and Robotics in 1997, at the Universidad Politécnica de Madrid (UPM). He is currently a Full Professor at UPM and a researcher at 'Centre for Automation and Robotics UPM-CSIC'. He has participated and coordinated several research projects in Robotics and Automatic Control, both at national and international programs. His research interest is focused on Automatic Control, Advanced Telerobotics, and Haptics. He has four patents of haptic devices and stereoscopic video cameras. He is author of more than 150 publications and editor of the 'Springer Series on Touch and Haptics System'.